

# **DEVELOPMENTAL ROLE OF EMBRYONIC CECA IN HINDGUT ENTERIC NERVOUS SYSTEM FORMATION**

**Ph.D. thesis**

**Tamás Kovács**

Semmelweis University Doctoral School  
Molecular Medicine Division



Supervisor: Nándor Nagy, D.Sc.

Official reviewers: Ágota Apáti, D.Sc.  
Mária Sótiné Bagyánszki, Ph.D.

Head of the Complex Examination Committee:  
Edit Buzás, D.Sc.

Members of the Complex Examination Committee:  
Attila Mócsai, D.Sc.  
Elen Gócza, D.Sc.

Budapest  
2026.

# **1. Introduction**

The enteric nervous system (ENS) is composed of more than 100 million enteric neurons and glial cells, organized into two plexuses – the myenteric and the submucosal plexus. During embryonic development, the cells that form ENS derive from the neural crest. Neural crest cells delaminate from the dorsal part of the neural tube and as a highly invasive multipotent stem cell population start their migration to almost every organ of the developing embryo. The neural crest cells reach the developing gut at the level of the foregut, enter into the mesenchyme (we call them enteric neural crest derived cells, ENCDCs from this point) and colonize the distalmost part of the colorectum.

Impaired ENCDC proliferation, migration or differentiation can lead to Hirschsprung disease (HSCR), which is characterized by an aganglionic distal bowel. Current treatments are limited to surgical resection of the aganglionic segment. However, postoperative morbidity following pull-through surgery remains a major problem, which highlights the need for improved therapies for HSCR. To develop a regenerative medicine approach utilizing stem cell-based therapy to treat HSCR we need to understand the genetics and molecular background of normal and pathological ENS development.

The avian embryo is a valuable model system for studying ENS: unlike mammals, the avian embryo allows for embryo manipulation experiments whose effects can be tracked in later stages of development, and developmental process in avian embryos closely resembles to human ENS development.

## 2. Objectives

Although the exact etiology of Hirschsprung disease (HSCR) remains unclear, recent decades have yielded significant insights into the complexity of this congenital neurointestinal disorder and its variants. Advances in our understanding of ENS development and the molecular and genetic regulation of neurointestinal disorders have revealed that HSCR is a genetically complex and heterogeneous illness. It arises from abnormal development of neural crest cells and involves multiple mutations across various genes and signaling pathways, besides other molecular factors that are yet to be fully identified.

### **The primary objectives of this thesis are:**

1. To characterize the role of the avian ceca in the development of the hindgut enteric nervous system using avian embryonic surgery techniques and molecular approaches.
2. To identify novel growth factors of cecal origin in hindgut ENS development and to experimentally validate their contribution to ENS formation.

### **My specific aims include:**

Characterizing the expression pattern of non-canonical **WNT5A** and **WNT11** together with **BMP4** during avian hindgut ENS development and investigating the effects of these pathways on the proliferation, migration and differentiation of enteric neural crest-derived cells and on colorectum ENS development.

### **3. Methods**

#### **3.1. Animals / Embryos**

Fertilized White Leghorn chicken (*Gallus gallus domesticus*) eggs were obtained from commercial breeders and maintained at 37.5 °C in a humidified incubator. Transgenic green fluorescent protein (GFP)-expressing chicken eggs were obtained from Prof. Helen Sang, The Roslin Institute, University of Edinburgh, UK. Embryos were staged according to the number of embryonic (E) days or to Hamburger and Hamilton (HH) tables. Gut stages were referenced to the chick embryo gut staging table and the ENS formation timetable.

#### **3.2. Histological techniques**

##### **3.2.1. Whole-mount immunostaining**

For the whole mount immunostaining procedure distal gut segments were used. The samples were fixed in 4% PFA overnight at 4°C. The gut segments were immersed in 12-well plates and permeabilized with 0.1% Triton-X PBS overnight at 4°C. The primary antibody ( $\beta$ 3-tubulin [Tuj1]) was diluted in 1:400 in PBS-BSA containing 1% goat serum. The gut segments were incubated with the primary antibody for 2 hours at room temperature, while shaking followed by an overnight washing step in PBS. The next day, the samples were incubated for 1 hour at room temperature, covered from light with the secondary antibody (goat anti-mouse IgG(H+L) AlexaFluor 488). After a brief washing the images were recorded with Nikon SMZ25 fluorescent stereomicroscope.

### **3.3. In situ hybridization**

#### **3.3.1. Whole-mount in situ hybridization**

Dissected gastrointestinal tracts were fixed in 4% paraformaldehyde (PFA), dehydrated in methanol, and stored at -20 °C until ready for processing. Published chick probes were used: Wnt5a, Wnt11, Fzd7, Bmp4. Digoxigenin riboprobe synthesis and whole-mount RNA in situ hybridization were performed.

#### **3.3.2. In Situ Hybridization on FFPE sections and on primary cell cultures**

For sections, embryonic gut segments were fixed in 4% PFA at room temperature for 1 hour, washed in PBS, gradually dehydrated in ethanol, and embedded in paraffin. Sections (10 µm) were cut using a microtome and collected on poly-L-lysine coated slides. All sections were hybridized for 18-24 hours. Detection was performed using BM purple, according to the manufacturer's instructions. Digoxigenin riboprobes were prepared as described by Riddle. Published chick probes were used for FFPE sections and for primary cell cultures: Bmp4, BMPRII, Fzd7.

### **3.4. Embryo manipulation techniques and ex vivo experiments**

#### **3.4.1. Ceca ablation and recombination chimera**

For ceca ablation experiments, ceca buds were separated from the midgut-hindgut segment of E6 (HH28) chicken embryonic guts by using Moria Pascheff-Wolff Spring scissors. The remaining intestinal segments were cultured in catenary dishes. For the recombination experiment, ceca buds were

removed from both GFP+ and non-GFP chick embryonic guts in the same manner. The ceca buds of the non-GFP chick embryo were replaced with ceca isolated from a GFP-chick embryo. The proximal-distal and left-right orientations were maintained during recombination. To allow the tissues to adhere, ceca and intestine recombinants were embedded in a 3D collagen gel matrix. After three days, chimeric guts were removed, and immunofluorescence was performed.

#### 3.4.2. Collagen gel culture

In the first step, 700  $\mu$ l of DMEM (Sigma), 6  $\mu$ l of 1 N NaOH, and 294  $\mu$ l of collagen (rat tail collagen I, 3.38 mg/ml; BD Biosciences, 354236) were added to an Eppendorf tube in the given order while keeping it on ice. 350  $\mu$ l from this solution was measured into a Falcon Center-Well Organ Culture Dish (Corning, 353037) and incubated for 5 minutes at room temperature and another 5-10 minutes at 37 °C in a CO<sub>2</sub> incubator until polymerization. The preparations were placed on top of the collagen layer and embedded with a second layer. The gut segments were cultured for 24-72 hours.

#### 3.4.3. Vital dye labeling

The vital lipophilic dye CellTracker CM-DiI (1,1'-dioctadecyl-3,3,3',3'-tetramethylindocarbocyanine perchlorate) was dissolved in DMSO at a concentration of 1 mg/ml. The concentrated stock of DiI solution was diluted 1:100 in 15% sucrose containing PBS as described earlier. To study the colonization of ceca-derived or interceca-derived ENCDCs in the hindgut, intestinal tracts dissected from E5.5 (HH27) chick embryos were injected with approximately 0.5  $\mu$ l DiI into the

ceca buds (n=9) and interceca mesenchyme (n=7). Microinjection was processed by using Nikon SMZ25 epifluorescence stereomicroscope.

#### 3.4.4. Intestinal organ culture assay

Embryonic chicken intestinal segments were collected in PBS containing penicillin-streptomycin under sterile conditions to prepare suspended, so-called catenary organ cultures. The sections were then attached to the bottom of sterile, non-toxic silicone-coated Petri dishes by using insect needles to suspend them in the surrounding liquid (culture media, DMEM) and prevent adhesion to the silicone. The cultures were maintained for 2 to 3 days.

#### 3.4.5. Viral overexpression

Retroviral vectors can be used to create targeted gain-of-function and loss-of-function mutations in avian embryos. The method involves amplifying a retroviral plasmid in *E. coli* strains, culturing it on embryonic fibroblast cell line DF1, concentrating the virus particles by ultracentrifugation, and injecting them into the mesenchyme of a specific intestinal segment of early chicken embryos. After being injected into the tissue, the virus infects dividing cells. The retrovirus is then incorporated into the genome of the newly formed cells. During our experiment, 2-5  $\mu$ l of BMP4-RCAS retrovirus suspension with 0.1% Fast Green solution in PBS was injected into the E6 chicken hindgut mesenchyme by using the Narishige brand microinjector, 100  $\mu$ l Hamilton syringe and thin glass capillary. The injected segments were further cultured on an E8 chick chorioallantoic membrane (CAM) for 9 days. Avian retroviruses

have a specific tropism for mesenchymal cells and do not directly target ENCDCs. The 3C2 antibody, which recognizes the RCAS P19 gag protein, indicates successful and extensive viral replication in the intestinal wall.

### **3.5. Primary cell culture and in vitro experiments**

#### **3.5.1. Cell migration assay**

For ENCDC migration assay, distal midgut without ceca and the cecal region was isolated from E6 (HH29) chick embryos and cultured on 20 µg/mL fibronectin coated plastic surface with GDNF (10 ng/mL) and GDNF in combination with different recombinant proteins (WNT11: 500 ng/mL; BMP4: 200 ng/mL or Noggin: 200 ng/mL) dissolved in DMEM culture medium.

#### **3.5.2. Cell proliferation, EdU labeling**

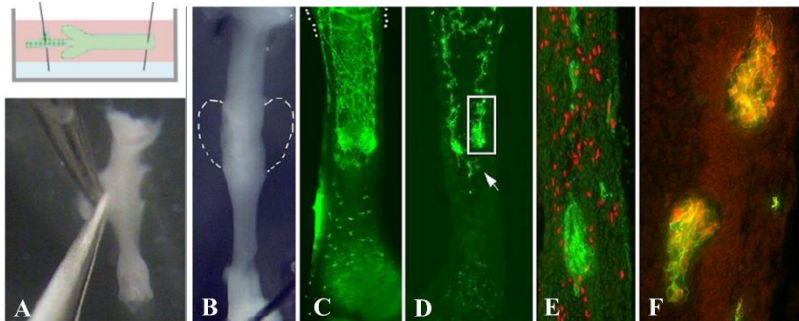
For cell proliferation, 5-ethynyl-2'-deoxyuridine (EdU) was added to the culture medium 2 or 3 hours before 4% PFA fixation. This can be used for direct measurement of *de novo* DNA synthesis or S-phase synthesis of the cell cycle by using click chemistry. Click chemistry is a method for covalently coupling of an azide with an alkyne. EdU incorporation was detected by using the Click-iT EdU Imaging Kit with Alexa Fluor 488 or 647 azides (Thermo Fisher Scientific, Click-iT EdU Proliferation Kit for Imaging). The developed fluorescent signals were examined under fluorescent or confocal microscope.



## 4. Results

### 4.1. Avian ceca are required for normal enteric nervous system development

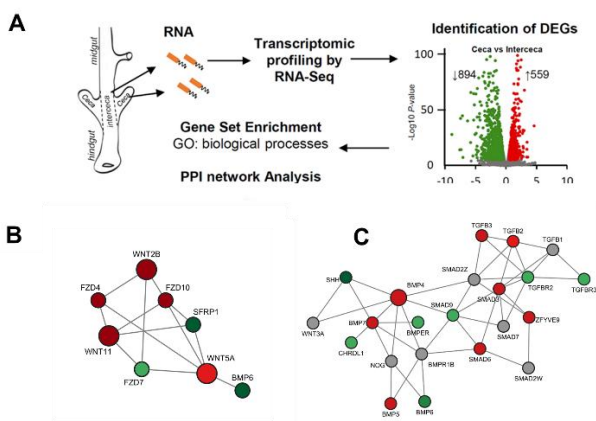
First, we quantified the number of proliferating ENCDCs at various stages at the level of migrating wavefront. Interestingly, the proliferation rate of ENCDCs peaked as the wavefront traversed through the cecal region at E6. The ENCDCs might receive a mitogenic signal here promoting their collective migration which necessitates a certain number of cells to continue their migration to the distal gut. To further investigate the role of ceca in ENS development, we microsurgeically removed (A) these paired pouches from the midgut-hindgut junction just before the colonizing ENCDCs reach this area. We cultured the segments in catenary organ culture, which mimics the *in vivo* like conditions. Compared to control gut segments, in case of ablated ceca we observed incomplete colonization of the hindgut (C), large ganglion-like cell aggregates on whole-mount with Tuj1 (D) and longitudinal sections stained with N-cadherin (E). Inside these cluster of cells no sign of proliferation (E, absence of red EdU+ signal) and premature differentiation was found (F) indicated by Tuj1 (green) and nNOS (red) double positivity.



To confirm our results from ablation studies we also performed tissue recombination, where we removed the ceca from E6 intestines and substituted them with GFP+ transgenic chicken derived ceca. GFP+ cells migrated out distally to populate the hindgut mesenchyme. Co-immunofluorescence showed that the hindgut ENS arised exclusively from ceca-derived GFP+ cells. Fluorescent lipophilic vital dye injection to cecal and intercecal mesenchyme resulted in similar results. We can conclude that hindgut ENCDCs arise from the ceca and not from the intercecal region or at least they have to pass through the cecal mesenchyme to be able to continue their migration.

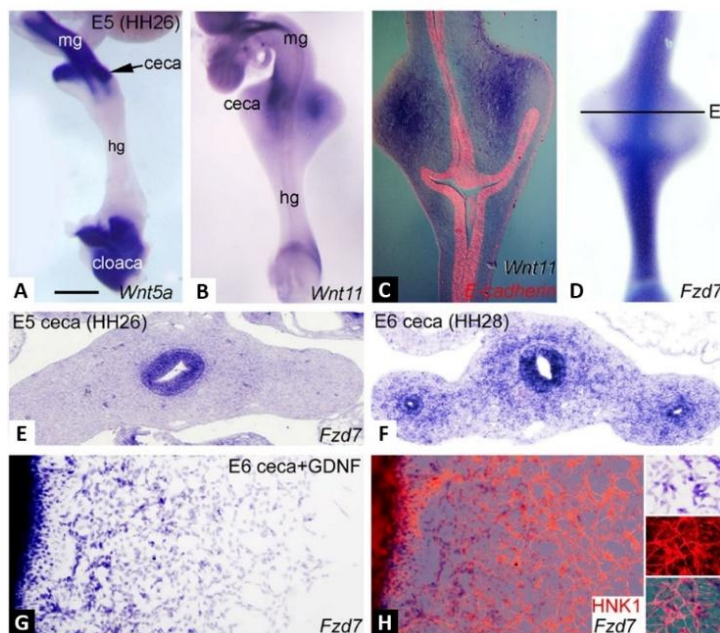
## 4.2. Identifying ceca derived factors as new important signaling cues in ENS formation of avian hindgut

To better understand what makes the ceca so unique for ENCDCs, we compared E5 ceca and interceca at transcriptomic level with bulk RNA-sequencing (A). Two signaling modules were specially enriched in the cecal tissue: the non-canonical WNT signaling (B) and BMP signaling elements (C).



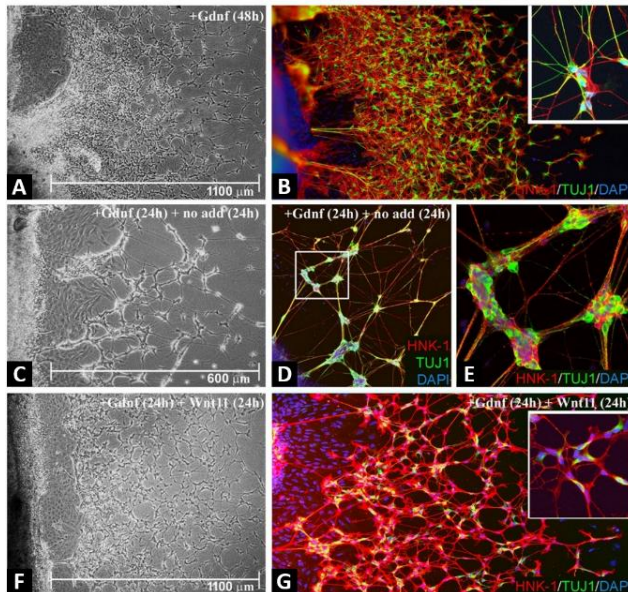
### 4.3. Expression of non-canonical planar cell polarity pathway genes in the ceca

Wnt pathway genes are expressed in the ceca and migrating ENCDCs. Whole-mount in situ hybridization (ISH) of E5 distal intestine shows Wnt5a expressed in the midgut, ceca and cloaca (A). Wnt11 is prominently expressed in the E5 ceca as demonstrated by wholemount ISH (B) and in a longitudinal section co-stained with an E-cadherin probe to delineate the epithelium (C). At E5, Fzd7 is expressed throughout the gut epithelium, apart from the cecal buds (D) and, at E6, Fzd7 is also expressed in the ceca and hindgut mesenchyme (data not shown). (G,H) Explanted E6 chick ceca were cultured with GDNF, which promotes significant ENCDC migration from the gut. Insets show an enlarged view of Fzd7-expressing ENCDCs.



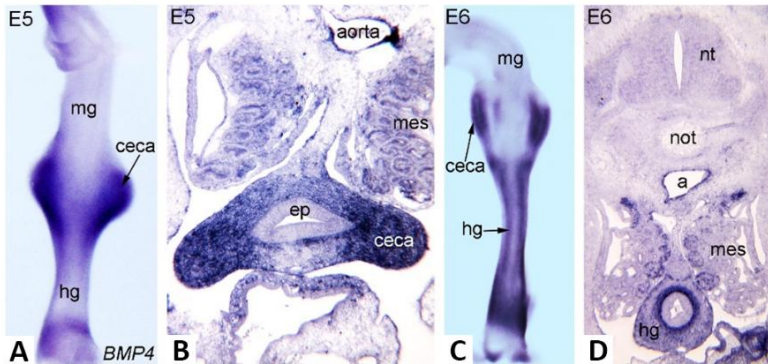
#### 4.4. WNT11 suppresses neuronal differentiation in the hindgut ENS

E6 ceca were cultured on fibronectin-coated plates with GDNF for 48 h and subsequently stained with HNK1 (red) and TUJ1 (green) antibodies (B) to evaluate ENCDC migration distance and neuronal differentiation. The magnified picture in the inset illustrates neuronal differentiation. In the cultures (C,F) GDNF was eliminated after the initial 24 hours, followed by an additional 24 hours with either no supplementary factors (C-E) or the addition of WNT11 protein (F,G). The inset in (E) displays a magnified view of the undifferentiated ENCDCs. E6 ceca were cultured with WNT11 protein alone with no migration of ENCDCs observed. The incorporation of WNT11 markedly suppressed neuronal differentiation of ENCDCs (data not shown).



#### 4.5. Expression of BMP signaling pathway genes in the ceca

The expression of BMP4 has been previously documented in the gastrointestinal system of vertebrates; however, its expression during the development of the avian hindgut and the formation of the ENS remained unknown. Whole-mount in situ hybridization was conducted shortly after ENCDCs colonized the post-umbilical midgut at stage E5 (A,B) and the ceca at stage E6 (C,D) to investigate the spatial pattern of BMP4 expression in the developing colorectum. The expression pattern of BMP4 was confined to the ceca mesenchyme on E5, whereas its appearance in the hindgut mesenchyme commenced only at stage E6. Later (E6-E14), the expression extends to the whole hindgut inner mesenchyme, but does not show co-expression with ENCDCs (data not shown).

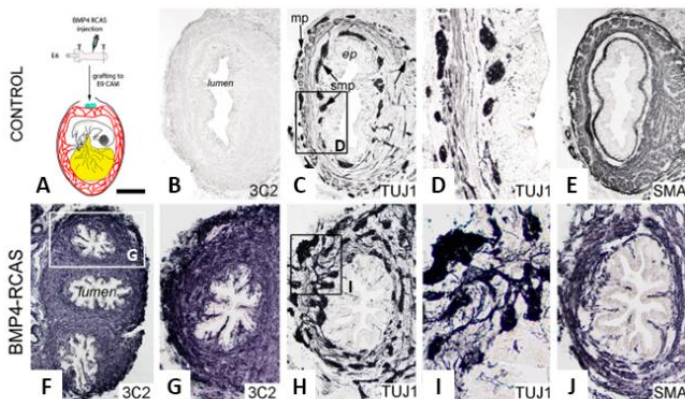


The expression of bone morphogenetic receptor type 2 (BMPR2) was also investigated with in situ hybridization technique at various developmental stages and we also confirmed the functional BMP activity at the same stages with an antibody, recognizing the active and phosphorylated form of SMAD1, 5, and 8. Interestingly, pSMAD expressions were

absent in ENDCs at the migratory wavefront. Later, when the migratory wavefront had reached the distal hindgut (E8), the enteric ganglia expressed pSMADs.

#### 4.6. The overexpression of BMP4 via retrovirus leads to extensive gangliogenesis

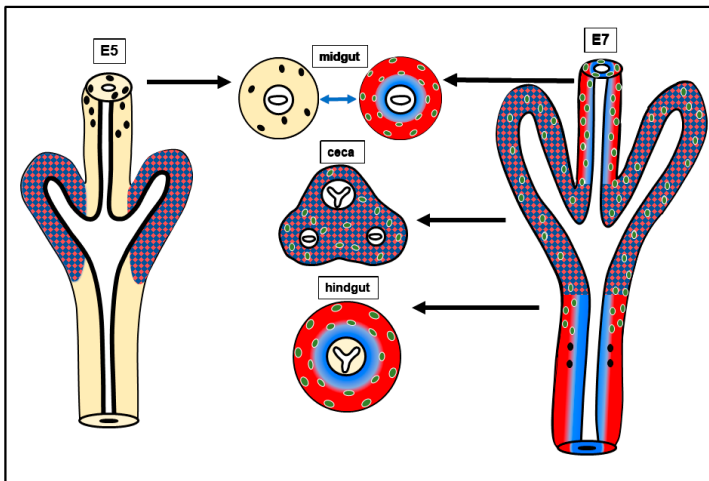
The influence of BMP4 on the development of the hindgut ENS was investigated *in vivo* utilizing a replication-competent retrovirus (RCAS) that expresses the chicken BMP4 gene. The RCAS virus was injected into the E6 chicken hindgut mesenchyme and subsequently cultured on E8 chick chorioallantoic membrane (CAM) for a duration of 9 days (A). The 3C2 antibody, which targets the RCAS p19 gag protein, demonstrates effective and widespread viral replication within the intestinal wall (F,G in comparison to B). RCAS-BMP4 induces substantial enteric hyperganglionosis, characterized by extensive and disorganized ganglia (I compared to D) throughout the gut wall, accompanied by the disruption of the unique organization into myenteric and submucosal plexuses (H) and smooth muscle layers (J) that is evident in the control intestine (C,E).





#### 4.7. Model of hindgut ENCDC colonization

We propose that the co-expression of BMP4 and GDNF is essential for hindgut ENS formation: GDNF counteracts the gangliogenic effect of BMP4 in the cecum, allowing wavefront cells to remain undifferentiated and continue migrating into the hindgut. Once past the ceca, ENCDCs enter a BMP4-free, GDNF-rich outer mesenchyme, where they differentiate and form enteric ganglia in the colorectum. WNT11, similarly restricted to the ceca, also inhibits premature neuronal differentiation, further ensuring that ENCDCs remain migratory and prevent early aggregation into ganglia-like clusters. This coordinated signaling mechanism ensures that a sufficient pool of undifferentiated progenitors reaches the distal gut to complete the ENS. Undifferentiated ENCDCs and wavefront cells are shown as black dots, differentiated ENS cells in green, mesenchymal compartment colored in yellow, while GDNF expression in red, and BMP4 expression in blue.



## 5. Conclusions

We observed that the proliferation of ENCDCs is high during their craniocaudal migration in the gut, particularly as the ENCDC wavefront goes across the ceca, which are a pair of pouches located at the midgut-hindgut junction in the avian intestine. Using avian embryo surgery and molecular analyses, we demonstrated that the cecal buds in the avian gut act as a critical staging area for enteric neural crest-derived cells (ENCDCs). With comparative transcriptome analysis of the cecal buds in comparison to the intercecal region we identified several cecal-derived growth factors that create a unique niche for the expansion of the undifferentiated ENCDCs and supporting their craniocaudal migration into the colorectum. In this cecal mesenchyme environment, ENCDC proliferation is promoted, while differentiation is inhibited, thereby maximizing the pool of undifferentiated progenitors available for hindgut colonization. Specifically, we characterized the expression and developmental biology roles of BMP4, WNT5A, and WNT11 in the developing avian hindgut, demonstrating their regulatory roles in ENCDC proliferation, migration, and differentiation, during development of the colorectum ENS. Our findings significantly contribute to understanding the key signaling pathways controlling ENCDC migration and differentiation, which are disrupted in enteric neurocristopathies, such as Hirschsprung disease. By integrating classical embryology and developmental biology methods as well as molecular biology studies, this research may contribute to new regenerative medicine approaches, leading to the development of more targeted, effective stem cell-based therapies.



## **6. Bibliography of the candidate's publications**

### **6.1. Publications related to the thesis:**

Nagy, N. *et al. Dev. Camb. Engl.* 148, dev199825 (2021)

**IF: 6.862**

Kovács, T. *et al. Int. J. Mol. Sci.* 24, 15664 (2023)

**IF: 4.900**

### **6.2. Publications not related to the thesis:**

Kudlik, G. *et al. Orv. Hetil.* 156, 1683–1694 (2015)

**IF: 0.291**

Dülk, M. *et al. Sci. Rep.* 6, 34280 (2016)

**IF: 4.259**

Dora, D. *et al. J. Anat.* 233, 401–410 (2018)

**IF: 2.638**

Vas, V. *et al. Sci. Rep.* 9, 5781 (2019)

**IF: 3.998**

Nagy, N. *et al. Development* dev.190900 (2020)

**IF: 6.862**

Dóra, D. *et al. Orv. Hetil.* 161, 771–779 (2020)

**IF: 0.540**

Mogor, F. *et al. Appl. Sci.* 11, (2021)

**IF: 2.838**

Dora, D. *et al. Cell. Mol. Gastroenterol. Hepatol.* 12, (2021)

**IF: 8.797**

Matula, Z. *et al. Cancers* 13, 3461 (2021)

**IF: 6.575**

Onódi, Z. *et al. J. Mol. Cell. Cardiol.* 165, 19–30 (2022)

**IF: 5.000**

Oláh, I. *et al. Poult. Sci.* 101, 101727 (2022)

**IF: 4.400**

Oláh, I. et al. *Anat. Rec.* Hoboken NJ 2007 305, 3297–3306 (2022)

**IF: 2.00**

Felföldi, B. et al. *Viruses* 14, 1689 (2022)

**IF: 4.700**

Gergely, T. G. et al. *Br. J. Pharmacol.* 180, 740–761 (2023)

**IF: 6.800**

Kucsera, D. et al. *Sci. Rep.* 13, 356 (2023)

**IF: 3.800**

Halasy, V. et al. *Dev. Camb. Engl.* 150, dev201289 (2023)

**IF: 3.700**

Dora, D. et al. *Oncoimmunology* 12, 2204746 (2023)

**IF: 6.500**

Ferenczi, S. et al. *Sci. Rep.* 13, 22451 (2023)

**IF: 3.800**

Kucsera, D. et al. *GeroScience* (2024)

**IF: 5.400**

Chen, Y. H. et al. *Br. J. Pharmacol.* (2024)

**IF: 7.700**

Sayour, N. V. et al. *ESC Heart Fail.* 12, 87–100 (2025)

**IF: 3.700**

Gergely, T. G. et al. *ESC Heart Fail.* 12, 1398–1415 (2025)

**IF: 3.700**

Sayour, N. V. et al. *Basic Res. Cardiol.* 120, 207–223 (2025)

**IF: 8.000**

Kovács, S. A. et al. *Br. J. Pharmacol.* 182, 3903–3922 (2025)

**IF: 7.700**

Hegedűs, Z. I. et al. *Cardiovasc. Diabetol.* 24, 253 (2025)

**IF: 10.600**

**Σ IF: 136.066**